AERIAL SMOOTHING IN RADIO ASTRONOMY

By R. N. BRACEWELL* and J. A. ROBERTS*

[*Manuscript received May* 17, 1954]

Summary

When an aerial is used to survey the distribution of radio brightness over the sky, the observed distribution is smoother than the true distribution ; the broader the beam of the aerial, the greater the smoothing. It is shown that the aerial does not register those spatial Fourier components of the true distribution having frequencies beyond a cut-off determined by the aerial aperture. Components of lower frequency are registered but their relative strengths are altered.

Two important consequences follow. (i) There are *invisible distributions* which produce no response when scanned by the aerial. Consequently there is not a unique solution to the problem of correcting for aerial smoothing. The established method of correcting by successive smoothing, leads to the *principal solution*, in which Fourier components accepted by the aerial have been restored to their full values, but the components rejected by the aerial are still not represented. (ii) In conducting a survey it is sufficient to observe at discrete intervals. The measuring points must be closer together than half the period of the Fourier component at cut-off. For an aperture of width w, this *peculiar interval* is equal to $\frac{1}{2}\lambda/w$ (radians).

I. INTRODUCTION

It is the objective of much radio-astronomical work to determine the intensity of the radio waves arriving at the Earth from different directions. For any one frequency and polarization the energy flux of this radiation field is conveniently specified by a distribution of brightness temperature over the celestial sphere. Such a description is appropriate since, in the régime where the Rayleigh-Jeans law holds, the brightness of a black body is directly proportional to the temperature.

One may be interested in the distribution of brightness temperature over the whole of the celestial sphere, a small area the size of the Sun, or, in the case of " radio stars ", over still smaller areas. In all cases, the aerials used tend to blur the detail of the distribution. The energy received when an aerial is pointed in a given direction is determined not by the brightness temperature in that direction alone, but by a weighted mean of the temperatures in all the directions contained within the aerial beam. If the aerial pattern is fine enough compared with the scale of the temperature distribution studied, then the observed distribution will approximate closely to the true distribution. Often this is not the case, and then the question arises whether, from an accurate knowledge of the aerial response, it is not possible to reconstruct the original distribution.

* Division of Radiophysics, C.S.I.R.O., University Grounds, Sydney.

It is known that certain types of smoothing process are reversible. For example, it is possible to recover daily sunspot numbers in full detail from daily values of the much smoother 30-day running means. The means must, however, be given without approximation. Aerial smoothing is so closely allied to smoothing by running means that one might surmise that the limit to detail obtainable from a survey with a given aerial could be improved indefinitely by increasing the accuracy of the observations and the closeness of their spacing.

In a number of investigations (Hey, Parsons, and Phillips 1948 ; Bolton and Westfold 1950) radio astronomers have attempted to reconstruct the original distribution which gave rise to their observations. A proposed restoration may be tested by smoothing it artificially with the known aerial directional diagram, and comparing the result with the observations. Good agreement is usually obtainable, and it has been thought that a restoration, so tested, must be a good approximation to the true distribution. This assumption now proves to be wrong, for it will be shown that there are always an infinite number of different restorations, all of which satisfy the test exactly.

A clear insight into the nature of the blurring produced by the aerial is obtained by studying the effect of the aerial on the spatial Fourier components of the temperature distribution. The true temperature distribution is supposed analysed into Fourier components, each being a sinusoidal temperature distribution of a certain strength and spatial frequency. The aerial affects these components by *eliminating* a semi-infinite band of high frequencies and altering the relative strengths of the lower frequency components. Thus, in the observed distribution the finest detail is irretrievably lost, while the less fine detail may be substantially modified.

The rejection of a semi-infinite band of high frequencies by the aerial is responsible for the existence of *invisible distributions*. These are distributions containing only frequencies which would be rejected by the aerial. They produce no response when scanned by the aerial. There is a great variety of such invisible distributions and consequently a great variety of distributions, each of which when smoothed by the aerial directional diagram reproduces the observed distribution. These possible solutions differ from each other only by the addition of invisible distributions.

To emphasize the importance of this effect two examples from the literature are shown in Figure 1. The radial distribution of brightness across the Sun at 21 cm obtained by Christiansen and Warburton (1953) is shown in Figure 1 (*a*). The authors state that, on the basis of their observations, they could not distinguish between the two very different distributions represented. In the second example (Fig. 1 (*b*)) the full line gives the distribution of 100 Mc/s cosmic noise along the galactic meridian passing through the galactic centre, as deduced by Bolton and Westfold (1950) from their measurements. In the same figure the broken line shows a (renormalized) distribution which according to Brown and Hazard (1953) gives the same result, when scanned with the aerial, as does the full curve.

This indeterminacy in the restoration of the observations made with aerials of finite resolving power seriously affects several important current investigations. One of these is the study of solar limb brightening, where there is a need for observations to compare with existing theories (e.g. Smerd 1950). As is suggested by Figure 1 (*a*), the peak brightness at the limb is not an appropriate quantity for comparison of theory and observation. Some sort of integral is more suitable. In another important investigation (Piddington 1951) the brightness of the galactic centre is taken from surveys on different frequencies over a 30 : 1 range, in order to ascertain a spectrum. The correction for aerial smoothing may here be of vital importance. The same serious problem would arise in determining the spectra of discrete sources from attempted measurements of the central brightness.

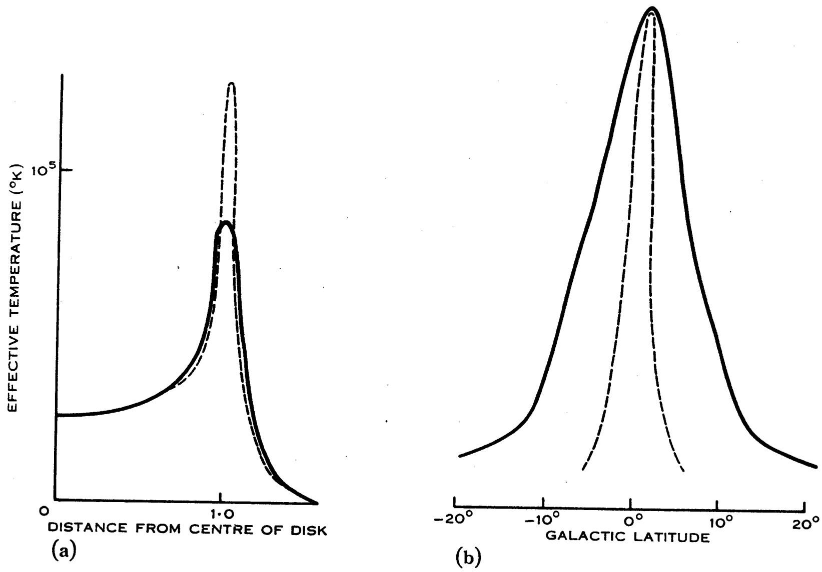

Fig 1 (*a*).—Solar distributions of brightness temperature (Christiansen and Warburton 1953) which could not be distinguished after subjection to aerial smoothing.

Fig. 1 (*b*).—A pair of similarly indistinguishable galactic distributions (Brown and Hazard 1953).

Given only the observations made with a finite aerial it is impossible to decide which of the feasible solutions is the true distribution. However, of those distributions which reproduce the observations when scanned by the aerial, the one which contains no invisible part has a certain uniqueness and is termed the *principal solution*. It is this distribution which is found when the observations are corrected by the process of successive substitutions (Section VIII). When the true distribution is well resolved by the aerial, the principal solution is a good approximation. However, if the true distribution is not well resolved, the principal solution may be a poor approximation, and even physically impossible.

To improve on the principal solution one must take into account further information about the distribution which may be available in particular cases. How best to do this in each case is an outstanding problem.

In Section VI we discuss a by-product of this investigation, namely, an important theorem which arises from the rejection of high frequencies by the aerial. There exists a critical angle, peculiar to each aerial, and such that no increase in information is obtained by making observations at finer intervals. In fact, from observations spaced at the peculiar interval, it is possible to infer the intermediate observations. This theorem is expected to be valuable both in the making and in the reduction of observations.

II. Basic Formula

For the present purpose of studying the effects of aerial smoothing and the possibilities of restoration, we shall discuss the simplest case, namely, when the brightness temperature $T(\varphi)$ depends on a single angular coordinate φ only. This case includes the essential physics of aerial smoothing and in fact covers many of the practical applications in radio astronomy.

It is convenient to specify the directional characteristics of the aerial by the power response $\mathbf{A}$ to a point source. Thus when the aerial beam is directed towards $\varphi=\varphi_0$ the response of the aerial to a point source at $\varphi=\beta$ is by definition proportional to $\mathbf{A}(\varphi_0-\beta)$. $\mathbf{A}$ is normalized so that

$$\int \mathbf{A}(\varphi)d\varphi=1.$$

It follows that the measured temperature distribution, $T_a(\varphi_0)$, corresponding to a point source of temperature T situated at $\varphi=\beta$ is given by

$$T_a(\varphi_0)=\mathbf{A}(\varphi_0-\beta)T.$$

The response to a point source, $\mathbf{A}(\varphi)$, is the power directional diagram, $A(\varphi)$, taken with φ in the opposite sense, i.e. $A(\varphi)=\mathbf{A}(-\varphi)$. For the development of the theory $\mathbf{A}$ proves to be more convenient than A, for reasons explained below. In many practical cases the directional diagram is symmetrical, so that the distinction need not be drawn.

When now the true temperature distribution $T(\varphi)$ is observed with the aerial pointed in the direction φ_0, the measured temperature $T_a(\varphi_0)$ will be a weighted mean of T given by

$$T_a(\varphi_0)=\int \mathbf{A}(\varphi_0-\beta)T(\beta)d\beta.$$

When the aerial is reasonably directive $\mathbf{A}(\varphi)$ becomes negligible beyond a small range of φ and the limits of integration may be extended to $\pm\infty$. For convenience, we also drop the subscript " 0 ", and thus obtain the equation

$$T_a(\varphi)=\int_{-\infty}^{\infty} \mathbf{A}(\varphi-\beta)T(\beta)d\beta. \quad \ldots\ldots\ldots\ldots\ldots \quad (1)$$

This equation expresses in its simplest form the phenomenon of aerial smoothing and forms the basis of the present communication. In other circumstances, the expression on the right-hand side of (1) would be known as the convolution, composition product, Faltung, fold, etc. of $\mathbf{A}(\varphi)$ and $T(\varphi)$ or as the (unnormalized) cross-correlation function of $\mathbf{A}(-\varphi)$ and $T(\varphi)$. To represent the convolution of two functions we shall use the abbreviated notation

$$\mathbf{A}*T\equiv\int_{-\infty}^{\infty}\mathbf{A}(\varphi-\beta)T(\beta)\mathrm{d}\beta\equiv\int_{-\infty}^{\infty}T(\varphi-\beta)\mathbf{A}(\beta)\mathrm{d}\beta,$$

and in this notation

$$T_a=\mathbf{A}*T.$$

We may also write

$$T_a=A\bigstar T,$$

where†

$$A\bigstar T\equiv\int_{-\infty}^{\infty}A(\beta-\varphi)T(\beta)\mathrm{d}\beta\equiv\int_{-\infty}^{\infty}T(\beta+\varphi)A(\beta)\mathrm{d}\beta.$$

In statistics $A\bigstar T$ would be called the (unnormalized) cross-correlation function of A and T.

III. Formal Solution by Fourier Transforms

Equations of the same type as (1) arise frequently in physics (see e.g. Trumpler and Weaver (1953) for references). Typical instances are the instrumental blurring of (i) optical spectra (van Cittert 1931 ; Burger and van Cittert 1932 ; van de Hulst 1941, 1946), (ii) X-ray spectra (Stokes 1948 ; Paterson 1950 ; Waser and Schomaker 1953), and (iii) solar limb darkening curves (Fellgett and Schmeidler 1952). A good survey of various methods of dealing with two-dimensional examples arising in astronomy is given by Burr (1955).

In the present application we make use of the special properties arising from the restriction of $\mathbf{A}(\varphi)$ to be the response of an aerial to a point source. For this class of problem the approach from Fourier theory is most enlightening. In this procedure the temperature distributions and the aerial pattern are regarded as built up of a spectrum of components harmonic in the angular variable φ. Thus $T_a(\varphi)$ is specified by its spectrum $\overline{T}_a(s)$ which is the (complex) Fourier transform of $T_a(\varphi)$ and gives the amplitude and phase of the harmonic component with s wave crests per unit of φ.

When functions are related as in equation (1) the corresponding relation between their Fourier transforms is very simple. This relation is given by the convolution theorem (Sneddon 1951) which can be stated in the form :

† Because the operation of convolution (denoted by $*$) is commutative ($f*g=g*f$), associative ($f*[g*h]=[f*g]*h$), and distributive ($[f+g]*h=f*h+g*h$) (Doetsch 1937), it may be treated algebraically like ordinary multiplication and thus leads to simple mathematics (Section VIII). On the other hand the operation of smoothing T with A (written $A\bigstar T$) is perhaps more direct for some purposes than forming the convolution $\mathbf{A}*T$ of $\mathbf{A}$ with T. In either case it is A which is plotted or tabulated when the calculation is performed. And, of course, A is the customary quantity in aerial physics, not $\mathbf{A}$. However, the smoothing process, being non-commutative and non-associative, proves to be not as convenient as convolution in the type of analysis occurring in the present paper.

If $\overline{T}_a(s)$ is the Fourier transform of $T_a(\varphi)$ defined by

$$\overline{T}_a(s)=\int_{-\infty}^{\infty} T_a(\varphi)\mathrm{e}^{-\mathrm{i}2\pi s\varphi}\mathrm{d}\varphi,$$

and, if $\overline{T}(s)$, $\overline{\mathbf{A}}(s)$ are similarly the transforms of $T(\varphi)$ and $\mathbf{A}(\varphi)$, then, when

$$T_a=\mathbf{A}*T,$$

the transforms are related by

$$\overline{T}_a(s)=\overline{\mathbf{A}}(s)\overline{T}(s). \quad\quad (2)$$

To state this theorem in words: if $T_a(\varphi)$ is obtained from $T(\varphi)$ by convolution with $\mathbf{A}(\varphi)$, then the Fourier transform of $T_a(\varphi)$ is the algebraic product of the transforms of $T(\varphi)$ and $\mathbf{A}(\varphi)$.

Equation (2) emphasizes the importance of zeros in the Fourier transform of the aerial diagram. Since $\overline{T}_a$ is obtained from $\overline{T}$ by multiplication with $\overline{\mathbf{A}}$, it follows that for those frequencies s_k for which

$$\overline{\mathbf{A}}(s_k)=0,$$

the value of $\overline{T}$ is lost in the smoothing process. For example, if $\overline{T}(s)$ contained a " spectral line " at $s=s_k$, $\overline{T}_a(s)$ would contain no trace of it.

For values of s such that $\overline{\mathbf{A}}(s)\neq 0$, the Fourier transform of the true distribution is given by

$$\overline{T}(s)=\frac{\overline{T}_a(s)}{\overline{\mathbf{A}}(s)}.$$

But when $s=s_k$, making both $\overline{\mathbf{A}}$ and $\overline{T}_a$ zero, equation (2) shows that $\overline{T}$ is indeterminate. Thus when $s=s_k$ equation (2) is satisfied not only by $\overline{T}(s)$ but also by

$$\overline{T}(s)+\sum_k a_k\delta(s-s_k),$$

where the a_k are arbitrary and $\delta(s-s_k)$ is unit impulse at $s=s_k$. It follows that $T(\varphi)$ is not the only solution of the integral equation ; it is also satisfied by

$$T(\varphi)+\sum_k a_k \mathrm{e}^{\mathrm{i}2\pi s_k\varphi}.$$

(If $\overline{\mathbf{A}}(s)$ is zero, not at discrete points, but over a continuous range, the summation is replaced by an integration.) The additive functions $\Sigma a_k \exp(\mathrm{i}2\pi s_k\varphi)$, which we term *invisible distributions* for the aerial, are obviously solutions of the integral equation

$$\int_{-\infty}^{\infty} \mathbf{A}(\varphi-\beta)T(\beta)\mathrm{d}\beta=0.$$

They are of such a nature that it is impossible to detect them with the aerial in question whatever their magnitude (see Section VI).

It is thus clear that the zeros of the transform of $\mathbf{A}(\varphi)$ play a vital role in the theory. For this reason it is now necessary to investigate the Fourier transforms of aerial patterns.

IV. Aerial Theory

In considering the nature of the Fourier transforms of aerial patterns in this section, we first illustrate their characteristics by discussion of a common type of aerial, and then establish a general theorem. For this purpose we regard the aerial as used for transmission or reception, whichever gives the simplest description, since the directional diagrams are identical in the two cases.

Thus for illustration consider an aerial consisting of a finite one-dimensional aperture of width w, across which is maintained a field constant in amplitude and phase. For this aerial the $\mathbf{A}(\varphi)$ for small φ is approximately

$$\mathbf{A}(\varphi)=\frac{\lambda}{w}\left\{\frac{\sin(\pi\varphi w/\lambda)}{\pi\varphi}\right\}^2,$$

the numerical factor being chosen so that $\int_{-\infty}^{\infty}\mathbf{A}(\varphi)d\varphi=1$. $\mathbf{A}(\varphi)$ is shown in Figure 2 (*a*). The beam width of the main lobe between zeros is $2\lambda/w$, the width to half power is $0\cdot 89\lambda/w$. Figure 2 (*b*) shows $\bar{\mathbf{A}}(s)$, the Fourier transform of

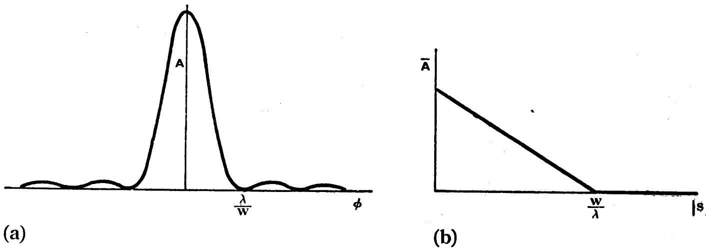

Fig. 2.—The response to a point source, $\mathbf{A}(\varphi)$, and its Fourier transform $\bar{\mathbf{A}}(s)$ for a uniformly illuminated aperture.

$\mathbf{A}(\varphi)$. Since $\bar{\mathbf{A}}(s)$ is real and symmetrical in this case, it may conveniently be plotted against $|s|$. (In subsequent figures illustrating transforms, we have, where convenient, taken them real and symmetrical.) The particular feature to notice is that $\bar{\mathbf{A}}(s)$ is zero for all values of s greater than the limiting frequency $s_c=w/\lambda$. We shall now show that this feature is common to all ordinary aerials consisting of finite plane apertures.

It is known (Booker and Clemmow 1950) that a one-dimensional aperture distribution of electric field $E(x/\lambda)$ and the angular spectrum $P(\sin\varphi)$ to which it gives rise are reciprocal Fourier transforms with respect to $\sin\varphi$ and x/λ, that is,

$$P(\sin\varphi)=\int_{-\infty}^{\infty}E\left(\frac{x}{\lambda}\right)e^{i2\pi(x/\lambda)\sin\varphi}d\left(\frac{x}{\lambda}\right),$$

and

$$E\left(\frac{x}{\lambda}\right)=\int_{-\infty}^{\infty}P(\sin\varphi)e^{-i2\pi(x/\lambda)\sin\varphi}d(\sin\varphi).$$

The angular spectrum $P(\sin\varphi)$ is proportional to the field directional diagram for real values of φ. When $|\sin\varphi|>1$, that is, for imaginary values of φ, $P(\sin\varphi)$ represents the evanescent field of the aerial, which is normally small for very directive aerials.* If we assume it to be negligible the power directional diagram $A(\varphi)$ is given by

$$\begin{aligned} A(\varphi) &= \text{const.}\ |P(\sin\varphi)|^2 \\ &= \text{const.}\ P^\dagger P, \qquad \ldots\ldots\ldots\ldots \quad (3) \end{aligned}$$

where $P^\dagger$ is the complex conjugate of $P \equiv P(\sin\varphi)$. The directional diagram $A(\varphi) = \mathbf{A}(-\varphi)$ is used here instead of $\mathbf{A}(\varphi)$, the response to a point source, to obtain agreement with the usual practice in aerial theory.

As a further consequence of the assumption of directive aerials, it is permissible to replace $\sin\varphi$ by φ in the equations above, since $P(\sin\varphi)$ is negligible where this approximation is invalid. Then applying the convolution theorem of Section III to equation (3) we have

$$\bar{A}(s) = \text{const.}\ \overline{P^\dagger} * \bar{P},$$

and with a little further reduction

$$\bar{\mathbf{A}}(s) = \text{const.}\ E \star E^\dagger.$$

Stating this important result in words, the Fourier transform of the aerial response pattern $\mathbf{A}(\varphi)$ is proportional to the (complex) auto-correlation function of the aperture distribution (see also Booker, Ratcliffe, and Shinn 1950).

For an aperture of width w, it follows that $\bar{\mathbf{A}}(s)$ is zero for frequencies greater than w/λ. This result is in obvious agreement with the discussion of the uniformly fed aperture above, but it extends this result to more general aerials.

We have not covered all aerials but we know from experience that the directivity of a broadside array cannot be exceeded very much by rearranging its elements within the same overall dimensions. In any particular case the existence of the cut-off could be verified and the value of s_c determined by taking the Fourier transform of the aerial diagram.

The highest frequency which can be present in $\mathbf{A}(\varphi)$, the cut-off frequency s_c, is given by

$$s_c = \frac{w}{\lambda}.$$

The inverse of this frequency

$$\varphi_c = \frac{1}{s_c}$$

may be termed the cut-off period. For a uniformly illuminated aperture it is half the beam width between zeros or 1·12 times the beam width to half power.

V. Aerial Smoothing

It has been shown in Section III, equation (2), that the effect of aerial smoothing may be described in terms of spectra by the statement that the spectrum of the observed temperature distribution T_a is obtained from the

* Very directive aerials with large evanescent fields have been mooted (see, for example, Woodward and Lawson 1948) but are of more theoretical than practical interest.

spectrum of the true distribution T by multiplication with the spectrum of the response of the aerial to a point source. But, according to the result of Section IV, the spectrum of any aerial response vanishes for all frequencies s beyond a limiting value s_c. The high frequency components of T are thus entirely rejected by the radiometer.

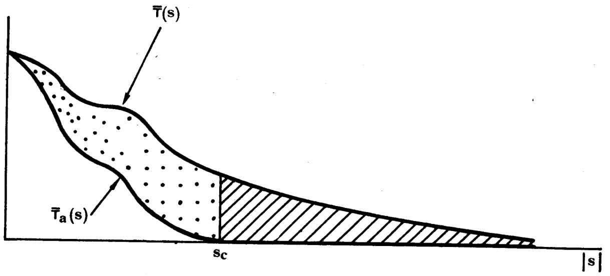

Fig. 3.—Showing how the spectrum of a smoothed distribution, $\bar{T}_a(s)$, is related to the spectrum of the original distribution $\bar{T}(s)$.

This is illustrated in Figure 3. $\bar{T}(s)$ is the spectrum of some $T(\varphi)$ which includes high frequencies. In $\bar{T}_a(s)$, the spectrum of the observed distribution, the whole of $\bar{T}(s)$ for frequencies greater than s_c (cross-hatched area) has been lost, and furthermore the lower frequency components have been reduced by the loss of the stippled area.

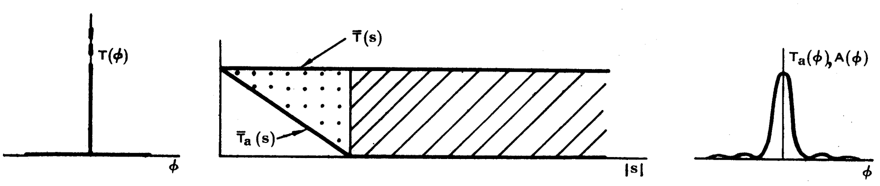

Fig. 4.—The effect of scanning a point source illustrated in terms of transforms.

Figure 4 gives the corresponding diagram for a point source scanned by an aerial consisting of a uniformly illuminated aperture for which

$$\mathbf{A}(\varphi)=\frac{1}{\pi}\left(\frac{\sin\varphi}{\varphi}\right)^2.$$

Since $T(\varphi)$ is an impulse function, its spectrum $\bar{T}(s)$ is flat (see Fig. 4). $\bar{T}_a(s)$, which contains none of the higher frequencies, and in which the lower frequencies have been reduced, is triangular as shown. $T_a(\varphi)$ has the same shape as $\mathbf{A}(\varphi)$, as is obvious.

Further illustrations of the spectral aspect of smoothing are given in Figure 5, which shows two cases of $T(\varphi)$, a rectangular distribution and a Gaussian error curve. Both true distributions are sufficiently broad, compared with the aerial beam, to be fairly well resolved.

In all cases $T_a(\varphi)$ is a distribution which contains no frequencies greater than a certain limit. This feature has important repercussions on the possibilities of restoration on the one hand and on the other hand has a practical bearing on the conduct of surveys. In the following section we discuss the properties of such " band-limited " functions.

VI. A Theorem Concerning Observed Distributions

Observed distribution functions $T_a(\varphi)$, by virtue of containing no frequencies greater than a limiting value s_c, have a property which is of great practical

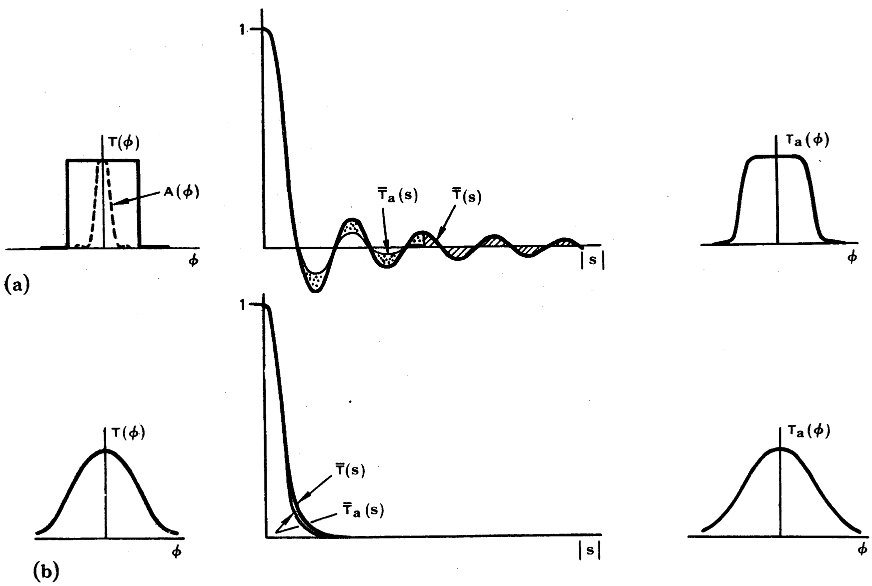

Fig. 5.—The effect of scanning (a) a rectangular and (b) a Gaussian source with the aerial pattern $A(\varphi)$.

significance. *An observed distribution is completely determined by measurements spaced at equal discrete intervals which are at least as narrow as* $\frac{1}{2}\varphi_c = \frac{1}{2}s_c^{-1}$. The interval $\frac{1}{2}\varphi_c$ is peculiar to the aerial used for the observations. For example, an aerial consisting of an aperture of overall width w has a peculiar interval of $\frac{1}{2}\lambda w^{-1}$, which in the case of a uniformly fed aperture is numerically equal to $0 \cdot 56$ times the beam width to half power. In this latter case also it is worth mentioning that the peculiar interval is just half the Rayleigh limit of resolution.

The peculiar interval theorem is analogous to one now well known in communication theory (see e.g. Shannon 1949). The proof given below is novel.

For the discussion of functions sampled at equal intervals of φ, it is convenient to define the improper function $\mathrm{III}(\varphi)$ which consists of an infinite sequence of unit impulse functions at unit separation, that is,

$$\mathrm{III}(\varphi) = \sum_{n=-\infty}^{\infty} \delta(\varphi - n).$$

This useful function is the same as the " row of impulses " of Heaviside (1922), who expressed it as the limit of a Fourier series. We find the symbol III convenient and pronounce it *shah* after the Cyrillic character. The function III has the simple and important property that its Fourier transform is also III. This is easily found by taking the limit of the Fourier *series* for a rectangular waveform. The transform of $\mathrm{III}(\varphi/b)$ is $b\mathrm{III}(bs)$. A further notation which is convenient when dealing with cut-off functions is $\Pi(s)$ for the even rectangle function of unit height and base ; $\Pi(s)$ is unity for $-\frac{1}{2}<s<\frac{1}{2}$, zero for $|s|>\frac{1}{2}$, and $\Pi(\pm\frac{1}{2})=\frac{1}{2}$. The function $\Pi(s/b)$ is a rectangle of unit height and base b and its Fourier transform is $(\pi\varphi)^{-1}\sin\pi b\varphi$.

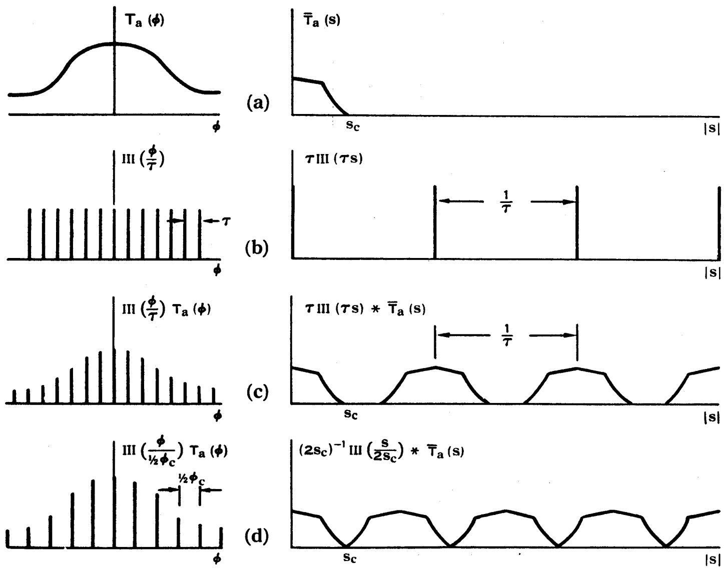

Fig. 6.—Several functions and their spectra, (*a*) an observed distribution, (*b*) a special sampling function, (*c*) sampling the distribution at discrete intervals is equivalent to multiplication by the sampling function, (*d*) sampling at the peculiar interval.

Samples taken at intervals τ from a function $T_a(\varphi)$ contain the same information as $\mathrm{III}(\varphi/\tau)T_a(\varphi)$. This function, which is a sequence of impulses at intervals τ and of strength proportional to $T_a(\varphi)$, is illustrated on the left in Figure 6 (*c*), impulse functions being shown as finite spikes of height proportional to their integral.

The Fourier transform of $\mathrm{III}(\varphi/\tau)T_a(\varphi)$ is $\tau\mathrm{III}(\tau s)*\overline{T}_a(s)$, that is, a function formed by repeating $\overline{T}_a(s)$ at intervals τ^{-1}. This follows from the convolution theorem, or it may be verified directly by calculating the Fourier coefficients of the periodic function $\mathrm{III}(\tau s)*\overline{T}_a(s)$. If T_a is sampled at sufficiently small intervals (τ sufficiently small) the spectrum of $\mathrm{III}(\varphi/\tau)T_a(\varphi)$ will consist of well-separated parts as shown on the right of Figure 6 (*c*). It is evident that, as long as τ^{-1} is greater than $2s_c$, that is, while the sampling interval τ is less than $\frac{1}{2}\varphi_c$, the separate parts will not overlap. Hence, when $\tau<\frac{1}{2}\varphi_c$, the exact spectrum of T_a is deducible from the spectrum of $\mathrm{III}(\varphi/\tau)T_a(\varphi)$, and therefore, finally, T_a itself is deducible from the values of T_a at intervals τ.

To recover T_a from $\mathrm{III}(\varphi/\tau)T_a(\varphi)$, it is merely necessary to remove all the Fourier components with frequencies beyond s_c, that is, to multiply the spectrum of $\mathrm{III}(\varphi/\tau)T_a(\varphi)$ by $\Pi(s/2s_c)$. By the convolution theorem this is equivalent to smoothing $\mathrm{III}(\varphi/\tau)T_a(\varphi)$ with $(\pi\varphi)^{-1}\sin 2\pi s_c\varphi$. Since $\mathrm{III}(\varphi/\tau)T_a(\varphi)$ is a sequence of impulse functions, the smoothing integral reduces, without approximation, to a summation.

In practice, interpolation midway between values of T_a given at the peculiar interval $\frac{1}{2}\varphi_c$ is the most frequently needed process. To do this, first prepare a table in which T_a appears in a column at unit intervals of $\Phi\equiv\varphi/\frac{1}{2}\varphi_c\equiv 2s_c\varphi$. Then tabulate $(\pi\Phi)^{-1}\sin\pi\Phi$ for $\pm\frac{1}{2}$, $\pm1\frac{1}{2}$, $\pm2\frac{1}{2}$, etc. in a strip thus :

1273
$\overline{2122}$
6366
$\longrightarrow$
6366
$\overline{2122}$
1273

the spacing being the same as in the table of T_a. The decimal points are omitted and negative values are indicated by bars. Table 1 gives further values. Place the strip alongside the T_a column, and the sum of the products of the adjacent numbers then gives the interpolated value of T_a opposite the arrow. To establish this procedure, put Φ=integer$+\frac{1}{2}$ and $\tau=\frac{1}{2}s_c^{-1}$ in the general equation for recovery of T_a. Thus

$$
\begin{aligned}
T_a &= \frac{\sin 2\pi s_c\varphi}{\pi\varphi} * \mathrm{III}\left(\frac{\varphi}{\tau}\right)T_a(\varphi) \\
&= \frac{\sin 2\pi s_c\varphi}{2\pi s_c\varphi} * 2s_c\mathrm{III}(2s_c\varphi)T_a(\varphi) \\
&= \sum_{\pm\Phi=\frac{1}{2},1\frac{1}{2},\ldots} \frac{\sin\pi\Phi}{\pi\Phi} T_a(\tfrac{1}{2}\varphi_c\Phi-\varphi).
\end{aligned}
$$

This property of the observed distributions, that they are sufficiently specified by spot values at intervals, is a direct consequence of the nature of aerial diagrams, and is obviously of great importance. For the observational programme it implies that (apart from the reduction of errors) nothing is gained by taking readings at intervals closer than $\frac{1}{2}\varphi_c=\frac{1}{2}s_c^{-1}=\frac{1}{2}\lambda w^{-1}$.

For computational work the property is equally important as it permits a band-limited function to be represented exactly by a set of discrete values. To ensure that data used in numerical work are in fact free from high frequencies, the data may be first " filtered " by smoothing with

$$\frac{\sin\pi\Phi}{\pi\Phi}.$$

TABLE 1

INTERPOLATING FUNCTION

$\|\Phi\|$	$\frac{\sin \pi\Phi}{\pi\Phi}$	$\|\Phi\|$	$\frac{\sin \pi\Phi}{\pi\Phi}$	$\|\Phi\|$	$\frac{\sin \pi\Phi}{\pi\Phi}$	$\|\Phi\|$	$\frac{\sin \pi\Phi}{\pi\Phi}$	$\|\Phi\|$	$\frac{\sin \pi\Phi}{\pi\Phi}$
$\frac{1}{2}$	0·6366	$7\frac{1}{2}$	−0·0424	$14\frac{1}{2}$	0·0220	$21\frac{1}{2}$	−0·0148	$28\frac{1}{2}$	0·0112
$1\frac{1}{2}$	−0·2122	$8\frac{1}{2}$	0·0374	$15\frac{1}{2}$	−0·0205	$22\frac{1}{2}$	0·0141	$29\frac{1}{2}$	−0·0108
$2\frac{1}{2}$	0·1273	$9\frac{1}{2}$	−0·0335	$16\frac{1}{2}$	0·0193	$23\frac{1}{2}$	−0·0135	$30\frac{1}{2}$	0·0104
$3\frac{1}{2}$	−0·0909	$10\frac{1}{2}$	0·0303	$17\frac{1}{2}$	−0·0182	$24\frac{1}{2}$	0·0130	$31\frac{1}{2}$	−0·0101
$4\frac{1}{2}$	0·0707	$11\frac{1}{2}$	−0·0277	$18\frac{1}{2}$	0·0172	$25\frac{1}{2}$	−0·0125	$32\frac{1}{2}$	0·0098
$5\frac{1}{2}$	−0·0579	$12\frac{1}{2}$	0·0255	$19\frac{1}{2}$	−0·0163	$26\frac{1}{2}$	0·0120	$33\frac{1}{2}$	−0·0095
$6\frac{1}{2}$	0·0490	$13\frac{1}{2}$	−0·0236	$20\frac{1}{2}$	0·0155	$27\frac{1}{2}$	−0·0116	$34\frac{1}{2}$	0·0092

VII. POSSIBILITIES OF RESTORATION

Having studied the nature of $\bar{\mathbf{A}}(s)$ for practical aerials we are now in a position to consider the solution of the integral equation (1). It follows immediately from the general discussions of Section III that there is no unique solution. From any known solution an infinite set of further solutions can be found by adding one of the invisible distributions. These are of the form $\int f(s) \exp (i2\pi\varphi s)ds$, where $f(s)$ is arbitrary and the integration extends over any values of s for which $\bar{\mathbf{A}}(s)$ is zero. These distributions produce no output when scanned by the aerial.

An infinite variety of such invisible distributions can be constructed. Those illustrated in Figure 7 are as follows: a harmonic distribution with spatial frequency beyond the cut-off frequency s_c; a "wave packet" containing only spectral components beyond cut-off; an impulse function from which the low frequencies have been removed; and a step distribution from which low frequencies have been removed.

In Figure 8 we have several solutions to a particular problem obtained by adding some of these distributions to an already known solution.

Since the invisible distributions contain no zero frequency component, they must all contain negative as well as positive values. In fact, to ensure that the aerial receives nothing, they must oscillate from positive to negative within the space of about one beam width. At first sight it would seem that distributions of this type could be disregarded as being physically implausible. However, when they are added to other particular solutions the result can be acceptable. In particular, the true distribution will contain some such invisible distribution whenever its spectrum extends to high frequencies.

In view of the lack of a unique solution to our problem, it may be asked whether any solution can be regarded as the most acceptable representation of the true distribution on the basis of the information available. In the past solutions have been obtained by methods of trial or iteration, using as a criterion of their approximation to the true distribution only that scanning them with the aerial should satisfactorily reproduce the observed curve. If there were only one solution, these methods would lead to it, but we now realize that in radio astronomy there are many solutions. Unawareness of this fact has led to false conclusions about the distribution of solar and galactic radiation.

If there is no knowledge of $T(\varphi)$ other than that contained in $T_a(\varphi)$, the most that can be done is to restore to their full value those (low frequency)

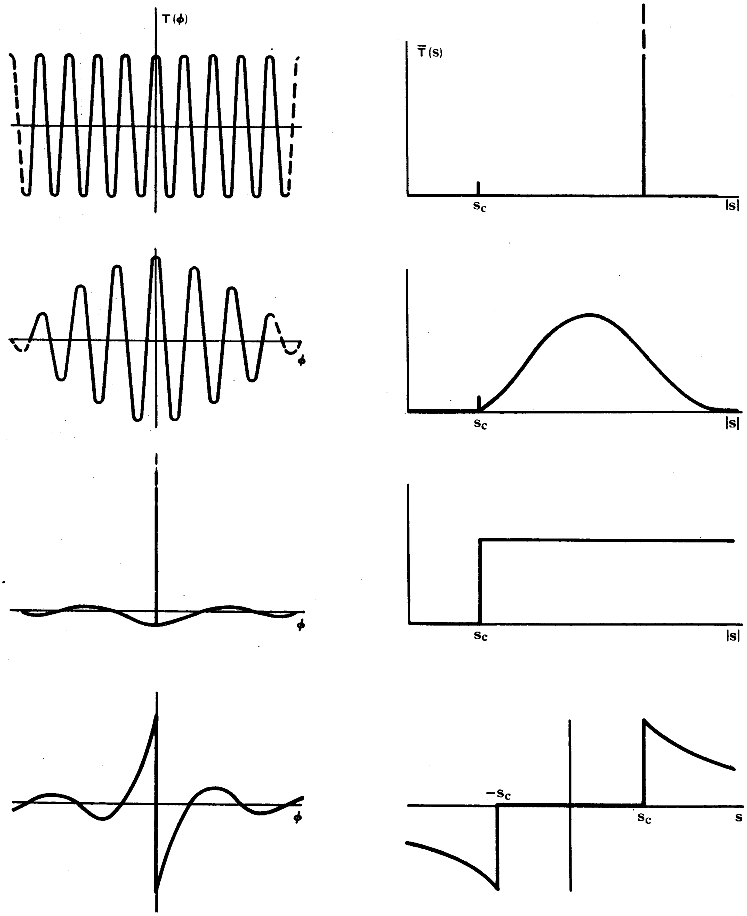

Fig. 7.—Some invisible distributions (left) and their spectra (right).

components of T which, while present in T_a, have been reduced in amplitude. This gives a unique result which we shall call the principal solution, $S(\varphi)$. We may define it as that solution whose spectrum is the same as the spectrum of the true distribution at all values of s for which $\bar{\mathbf{A}}(s)\neq 0$, that is,

$$\left.\begin{aligned}\bar{S}(s)&=\frac{\bar{T}_a(s)}{\bar{\mathbf{A}}(s)}, \qquad (\bar{\mathbf{A}}(s)\neq 0)\,;\\ &=0, \qquad\qquad (\bar{\mathbf{A}}(s)=0).\end{aligned}\right\} \quad \ldots\ldots\ldots\ldots \quad (4)$$

Figure 9 illustrates this for a typical aerial.

When there are no errors, the information contained in $\bar{S}$ is exactly the same as that given by an interferometer consisting of two aerials used at all spacings from zero up to the aerial width. However, the interferometer gives

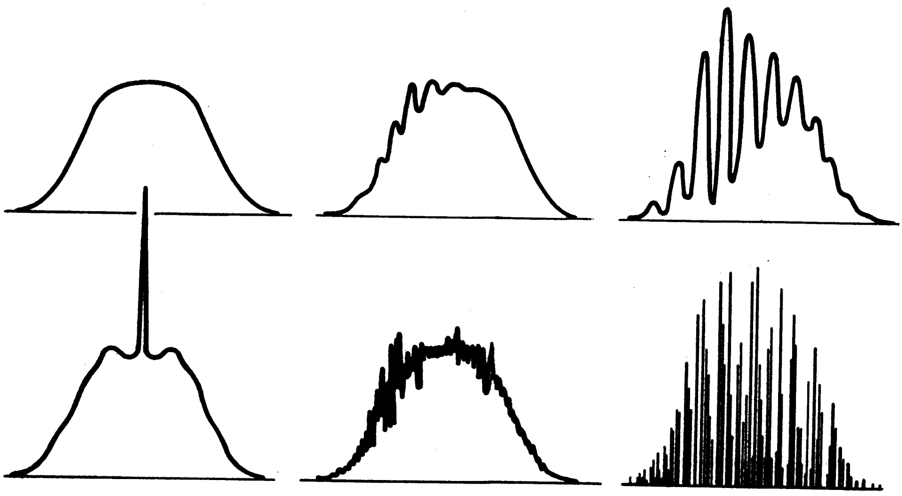

Fig. 8.—A variety of distributions which when scanned with the same aerial all give the same result.

the Fourier components of T directly at their full value, whereas the aerial reduces the components so that they must subsequently be restored. As components

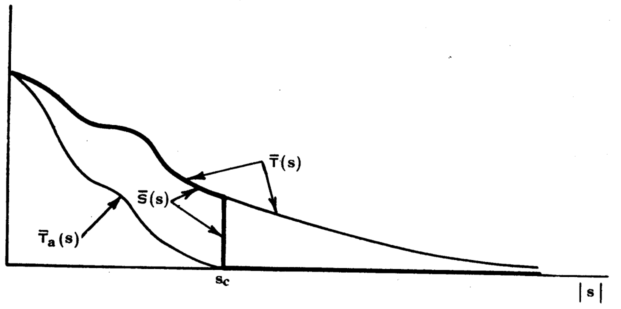

Fig. 9.—The relation between $\bar{S}(s)$ and $\bar{T}(s)$ for an aerial consisting of a uniform aperture.

near the cut-off frequency are very considerably reduced, the corresponding restored values in $\bar{S}$ are subject to very large errors. With this proviso the discussion below of solutions derived from $\bar{S}$ applies equally to the cases of an aerial and of an interferometer with variable spacing.

The degree of approximation of the principal solution to the true distribution depends markedly on the form of T. Thus when T contains no spectral components at those frequencies for which $\bar{\mathbf{A}}$ is zero, S is identical with T. However, when the spectrum of T is still appreciable at the cut-off frequency s_c, the resulting discontinuity in the spectrum of the principal solution can cause spurious oscillations in S. The effect of such a discontinuity is illustrated in Figure 10 where the principal solution is shown for two examples of $T(\varphi)$, an impulse function and a rectangular distribution. In both cases the principal solution has implausible oscillations, and indeed negative values which, in radio astronomy, are not physically possible.

When the principal solution is not a good approximation to the true distribution, three general methods are available for deriving a physically acceptable distribution which is an approximation to T. In the first approach the discontinuity in $\bar{S}$, which is responsible for the spurious oscillations in the

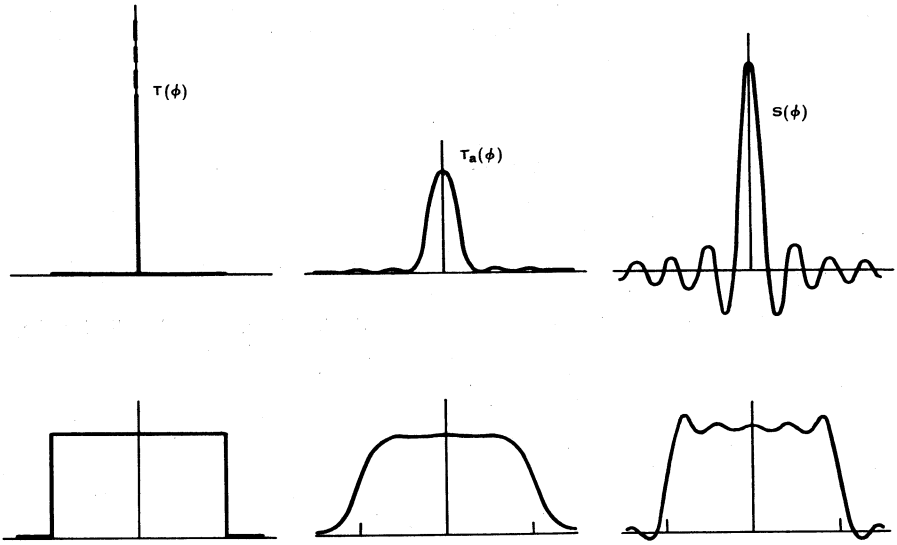

Fig. 10.—Cases where the principal solution $S(\varphi)$ is physically impossible.

solution, is changed to a smooth transition by reducing all the components below s_c by some suitable weighting function. This procedure yields a less oscillatory distribution, but at the expense of sharpness. It is commonly used in crystallography (Waser and Schomaker 1953) where the advantage of removing spurious maxima is considered to outweigh the disadvantage of loss of detail. (The information obtained from X-ray or electron diffraction is analogous to that obtained in radio astronomy with a two-aerial interferometer of variable spacing.) In radio astronomy the observed distribution T_a may be regarded as the result of applying such a weighting function, as is illustrated in Figure 9 ; the method of restoring by successive substitutions discussed in Section VIII is a method of successively reducing the severity of the weighting factor (Fig. 11).

A second approach, also sometimes used in crystallography, is to extrapolate the restored spectrum $\bar{S}$ to frequencies beyond the cut-off. The method has the advantage that no detail present in $\bar{S}$ is discarded. However, detail put in by extrapolation must be treated with due caution. In radio astronomy this method has been used to some extent with variable spacing interferometers (O'Brien 1953).

A further method is to construct families of physically plausible distributions and to match their spectra to $\bar{S}(s)$. The form of the trial distributions can be chosen so that the number of parameters to be fitted is as great as the knowledge of $\bar{S}(s)$ allows. This method has the advantage of using not only all the information available in $\bar{S}(s)$, but also any circumstantial knowledge of the true distribution. In practice one may fit either the spectra, or the values obtained at the sampling points when the trial solutions are scanned by the aerial.

The former case arises when variable spacing interferometers are used. An example is furnished by the attempts to find the diameter of the radio stars. Thus Smith (1952) measured $\bar{S}(s)$ for Cassiopeia and Cygnus and expressed his results in terms of the uniform disk whose spectrum agreed best with the observations. This unexceptionable procedure has much to recommend it, especially when, as in this case, a small number of parameters is deemed adequate to describe the measurements. The statement of the result contains a clear indication of the uncertainty.

VIII. Restoration by Successive Substitutions

One of the restoration procedures which has already been used in radio astronomy is equivalent to solving the integral equation of Section III by the method of successive substitutions (see e.g. Lovitt 1950). We study it here for its interest as a current procedure and its importance as a way of finding the principal solution. The process can be understood as follows. Suppose T_{app} is some approximation to T. Then it can be tested by scanning it with the aerial and comparing the result with T_a. The discrepancy $(T_a - \mathbf{A}*T_{app})$ is taken as a first estimate of the difference between T_{app} and T. This leads to a further approximation

$$T_{app}+(T_a-\mathbf{A}*T_{app}). \quad \dots\dots\dots\dots\dots\dots \quad (5)$$

If T_a itself is taken as the initial approximation to T one obtains as the first approximate restoration

$$T_1=T_a+(T_a-\mathbf{A}*T_a).$$

By applying the same procedure to T_1 we have a second restoration

$$T_2=T_1+(T_a-\mathbf{A}*T_1),$$

and the nth restoration is derived from the $(n-1)$th by the formula

$$T_n=T_{n-1}+(T_a-\mathbf{A}*T_{n-1}).$$

In practice the iteration is halted when smoothing the trial distribution with the aerial gives a result agreeing with T_a within the experimental error.

The approximate solution (5) can be written in two alternative useful forms. In the first form

$$T_n=T_a+\varepsilon_1+\varepsilon_2+\dots+\varepsilon_n, \quad \dots\dots\dots\dots \quad (6)$$

where

$$\varepsilon_1=T_a-\mathbf{A}*T_a=(\delta-\mathbf{A})*T_a,$$

$$\varepsilon_2=(\delta-\mathbf{A})*\varepsilon_1,$$

etc., the successive correction terms being obtained by convolution of the preceding correction with $\delta-\mathbf{A}$. In practice, operation on the correction term obviates the necessity for comparison with T_a as required in the form (**5**). In the second alternative form the relation is expressed in terms of successive smoothings of the observed distribution:

$$T_1=2T_a-\mathbf{A}*T_a,$$

$$T_2=3T_a-3\mathbf{A}*T_a+\mathbf{A}*\mathbf{A}*T_a,$$

$$\mathrm{T}_{n-1}=nT_a-\binom{n}{2}\mathbf{A}*T_a+\binom{n}{3}\mathbf{A}*\mathbf{A}*T_a+\ldots+\mathbf{A}^{*(n-1)}*T_a, \quad \ldots . \quad (7)$$

where $\mathbf{A}^{*n}=\mathbf{A}*\mathbf{A}*\ldots*\mathbf{A}$, the $\mathbf{A}$ appearing n times. van Cittert (1931) obtained the formula in essentially this form.

This elegant procedure, by which one restores smoothed out detail by further smoothing, appears to have been introduced into astronomy by van Cittert (1931) in connexion with the instrumental broadening of spectra. Bolton and Westfold (1950), and (in less explicit form) Hey, Parsons, and Phillips (1948), applied it in radio astronomy to correct their surveys of galactic radiation. It has since been used in other radio-astronomical applications.

Bolton and Westfold thought they had proved that the sequence of successive distributions converged to the true distribution. But, as we have shown, it is in general not possible to recover the true distribution from the observed one. We have therefore studied the process and find (i) that the sequence of distributions does not always converge to a limit and (ii) that when it does the limit is the principal solution defined in Section VII. Whilst developing the proof which follows we had the benefit of a discussion with E. J. Burr.

The Fourier transform of the nth restoration is, by equation (**6**),

$$\overline{T}_n(s)=\{1+[1-\overline{\mathbf{A}}(s)]+[1-\overline{\mathbf{A}}(s)]^2+\ldots+[1-\overline{\mathbf{A}}(s)]^n\}\overline{T}_a(s). \quad \ldots (8)$$

The series enclosed in braces may be recognized as the first $n+1$ terms of the binomial expansion of $\{1-[1-\overline{\mathbf{A}}(s)]\}^{-1}$. Hence, provided that $|1-\overline{\mathbf{A}}(s)|<1$,

$$\lim_{n\to\infty}\overline{T}_n(s)=\frac{\overline{T}_a(s)}{\overline{\mathbf{A}}(s)}.$$

This condition for the convergence of the binomial expansion is not met when $s=s_k$ since $\overline{\mathbf{A}}(s_k)=0$; but in that case $\overline{T}_n(s)$ is zero for all n since $\overline{T}_a(s)$ is itself zero (equation (**8**)). Therefore, when $|1-\mathbf{A}(s)|<1$ for all $s\neq s_k$, $\overline{T}_n(s)$ tends to the spectrum of the principal solution (equation (**4**)), and T_n tends to the principal solution.

This sufficient condition is met by many aerials. For example, in the case of symmetrical aerials, for which $\overline{\mathbf{A}}(s)$ is real, the condition amounts to requiring $\overline{\mathbf{A}}(s)$ to be non-negative and <2. Now $\overline{\mathbf{A}}(s)$ cannot exceed 1 on account of the normalization of $\mathbf{A}(\varphi)$. Hence it is sufficient that a symmetrical aerial have $\overline{\mathbf{A}}(s)$ non-negative in order that restoration by successive substitutions should converge to the principal solution whatever the form of T_a.

It should be noted, however, that $|1-\overline{\mathbf{A}}(s)|<1$ for $s\neq s_k$ is a sufficient condition. It is not a necessary condition; consequently convergent results may be obtained in cases where aerials do not obey it for all values of s, namely, where $\overline{T}_a(s)$ is zero at those values. Should cases of this sort become important, each T_a would have to be examined individually for convergence. The possibility

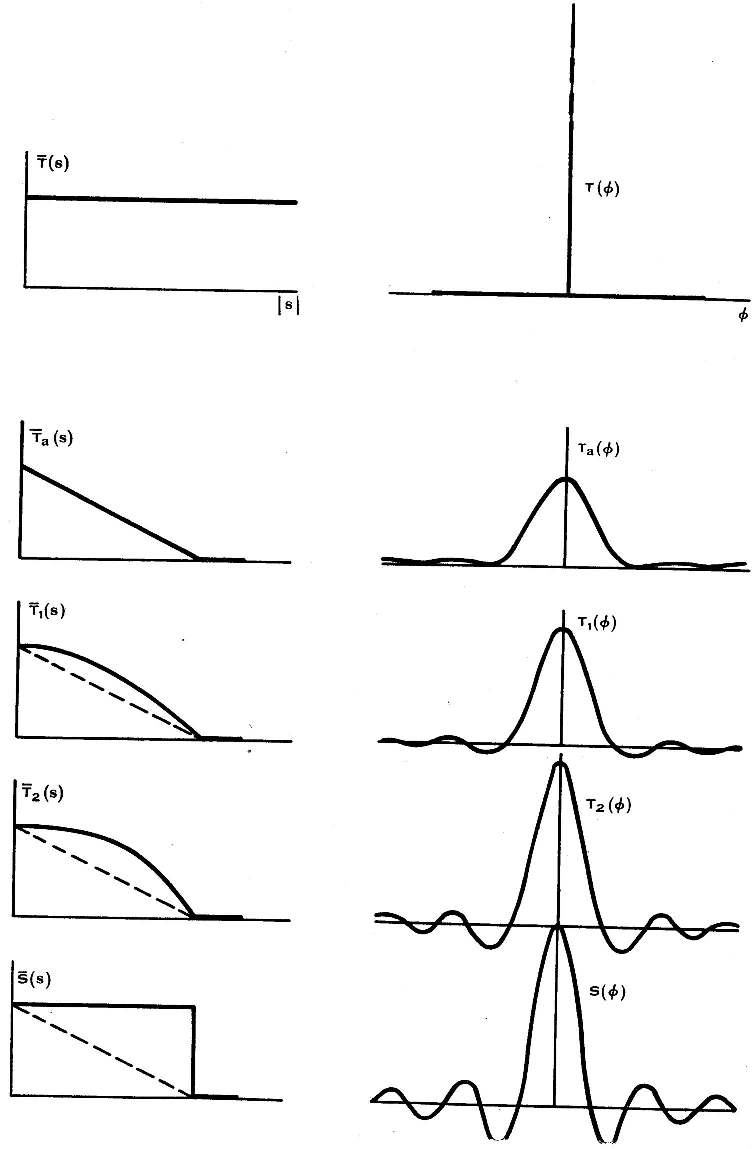

Fig. 11.—Successive restorations (right) of a point source, and their spectra (left).

of T_n approaching S asymptotically, even though ultimately divergent, would also become important.

To summarize, the necessary and sufficient condition for convergence is that $|1-\overline{\mathbf{A}}(s)|<1$ for all s such that $\overline{T}_a(s)\neq 0$.

The convergence of $T_n(\varphi)$ to the principal solution is illustrated in Figure 11 for the case of a point source scanned by an aerial consisting of a uniformly illuminated aperture. It is seen that the restorations tend towards a distribution of the form $\varphi^{-1}\sin\varphi$, which was shown above (Fig. 10) to be the principal solution for this case.

For any $T(\varphi)$ the spectra on the left may be interpreted as factors which, when multiplied into $\overline{T}(s)$, give $\overline{T}$, $\overline{T}_a$, $\overline{T}_1$, $\overline{T}_2$, . . ., $\overline{S}$; the distributions on the right, on convolution with $T(\varphi)$, give T, T_a, T_1, T_2, . . ., S. The distributions on the left may be regarded as weighting functions, in the sense of Section VII; the graphs of T_a, T_1, and T_2 show that the reduction of the spurious oscillations by drastic weighting is offset by broadening and lowering of the central peak. The distributions on the right may be interpreted as the point source responses of hypothetical aerials, which, if used to survey a temperature distribution, would yield T, T_a, T_1, etc. as the observed distribution.

Several stages of restoration may be performed in a single smoothing operation. It is evident from the forms (**6**) and (**7**) that we may write

$$T_n=R_n*T_a,$$

where the n-fold restoring distribution R_n is given by

$$R_n=\delta+(\delta-\mathbf{A})+(\delta-\mathbf{A})^{*2}+\ldots+(\delta-\mathbf{A})^{*n},$$

or by

$$R_n=(n+1)\delta-\binom{n+1}{2}\mathbf{A}+\binom{n+1}{3}\mathbf{A}^{*2}-\ldots(-)^n\mathbf{A}^{*n}.$$

For theoretical purposes R_n may be usefully expressed in the closed form

$$R_n=\mathbf{A}_i*[\delta-(\delta-\mathbf{A})^{*(n+1)}],$$

where $\mathbf{A}_i$, the inverse of $\mathbf{A}$, is defined by $\mathbf{A}_i*\mathbf{A}=\delta$. Notice that R_n does not in general approach a limit as n tends to infinity. When it is known how many stages of restoration are likely to be justified, it is possible to go direct to the nth restoration by using this formula. However, one should guard against over-restoration which leads simply to an enhancement of errors. In Table 2 we give the restoring distributions R_2 and R_3 for a uniform aperture.

In this case

$$A(\Phi)\equiv\mathbf{A}(\Phi)=\tfrac{1}{2}\left(\frac{\sin\frac{1}{2}\pi\Phi}{\frac{1}{2}\pi\Phi}\right)^2$$

$$=\begin{cases}2\pi^{-2}\Phi^{-2}, & \Phi \text{ odd},\\ \tfrac{1}{2}, & \Phi \text{ zero},\\ 0, & \text{other integral } \Phi.\end{cases}$$

The normalizing factor makes $\Sigma\mathbf{A}=1$. Table 2 also contains $\mathbf{A}$, $\mathbf{A}^{*2}$; and $\mathbf{A}^{*3}$.

If for any reason T_a contains frequencies beyond the cut-off these will be enhanced $n+1$ times in the nth stage of restoration, as can be shown from the form (**7**). T_a may contain high frequencies due to errors, or high frequencies may be introduced by initiating the restoration process with a trial solution which contains high frequencies. To avoid the enhancement of such spurious

TABLE 2

THE RESTORING FUNCTIONS R_2 AND R_3 FOR A PLANE APERTURE FED UNIFORMLY AND IN PHASE. THE RESPONSE TO A POINT SOURCE **A** AND ITS SUCCESSIVE SELF-CONVOLUTIONS $\mathbf{A}^{*2}$ AND $\mathbf{A}^{*3}$ ARE ALSO TABULATED

$\|\Phi\|$	**A**	$\mathbf{A}^{*2}$	$\mathbf{A}^{*3}$	R_2	R_3
0	0·5000	0·3333	0·2500	1·8333	2·0833
1	0·2026	0·2026	0·1808	—0·4053	—0·5861
2	0·0000	0·0507	0·0760	0·0507	0·1267
3	0·0225	0·0225	0·0323	—0·0450	—0·0773
4	0·0000	0·0127	0·0190	0·0127	0·0317
5	0·0081	0·0081	0·0120	—0·0162	—0·0282
6	0·0000	0·0056	0·0085	0·0056	0·0141
7	0·0041	0·0041	0·0062	—0·0083	—0·0144
8	0·0000	0·0032	0·0048	0·0032	0·0079
9	0·0025	0·0025	0·0037	—0·0050	—0·0087
10	0·0000	0·0020	0·0030	0·0020	0·0051
11	0·0017	0·0017	0·0025	—0·0033	—0·0058
12	0·0000	0·0014	0·0021	0·0014	0·0035
13	0·0012	0·0012	0·0018	—0·0024	—0·0042
14	0·0000	0·0010	0·0016	0·0010	0·0026
15	0·0009	0·0009	0·0014	—0·0018	—0·0032
16	0·0000	0·0008	0·0012	0·0008	0·0020
17	0·0007	0·0007	0·0011	—0·0014	—0·0025
18	0·0000	0·0006	0·0009	0·0006	0·0016
19	0·0006	0·0006	0·0008	—0·0011	—0·0020
20	0·0000	0·0005	0·0008	0·0005	0·0013
21	0·0005	0·0005	0·0007	—0·0009	—0·0016
22	0·0000	0·0004	0·0006	0·0004	0·0011
23	0·0004	0·0004	0·0006	—0·0008	—0·0014
24	0·0000	0·0004	0·0005	0·0004	0·0009
25	0·0003	0·0003	0·0005	—0·0006	—0·0011
26	0·0000	0·0003	0·0005	0·0003	0·0008
27	0·0003	0·0003	0·0004	—0·0006	—0·0010
28	0·0000	0·0003	0·0004	0·0003	0·0007
29	0·0002	0·0002	0·0004	—0·0005	—0·0008
30	0·0000	0·0002	0·0003	0·0002	0·0006

components, it is therefore necessary to filter the initial data as outlined in Section VI. Then the numerical work should be carried out at the critical interval to prevent the introduction of further high frequencies during the calculations.

IX. Application to the Quiet Sun

(a) *Data*

In this section the foregoing theory is illustrated for a practical case. The $\mathbf{A}(\varphi)$ is that of the central beam of the high-resolution aerial developed by Christiansen (1953) and is closely of the form $\varphi^{-2}\sin^2\varphi$. It has a beam width to half power of 3 min of arc and a beam width between zeros of 6·50 min. The peculiar interval $\frac{1}{2}\varphi_c$ is therefore 1·62 min. The angle φ measured in units of this peculiar interval is denoted as before by Φ. Integral values of Φ are then sufficiently closely spaced to define the band-limited functions. In terms of this normalized angle the aerial response is that given in the second column of Table 2.

For the observed distribution T_a we are indebted to Dr. Christiansen for providing a graph representing the quiet Sun (see the thin curve of Fig. 13). From this graph we have read off T_a at intervals to obtain Table 3. T_a is symmetrical, and zero outside the range given. The limits of error quoted were $\pm 0 \cdot 020\ (\Phi < 10)$ and $\pm 0 \cdot 030\ (\Phi > 12)$ whilst, on the steep portion $10 < \Phi < 12$, Φ was subject to error up to $\pm 0 \cdot 2$.

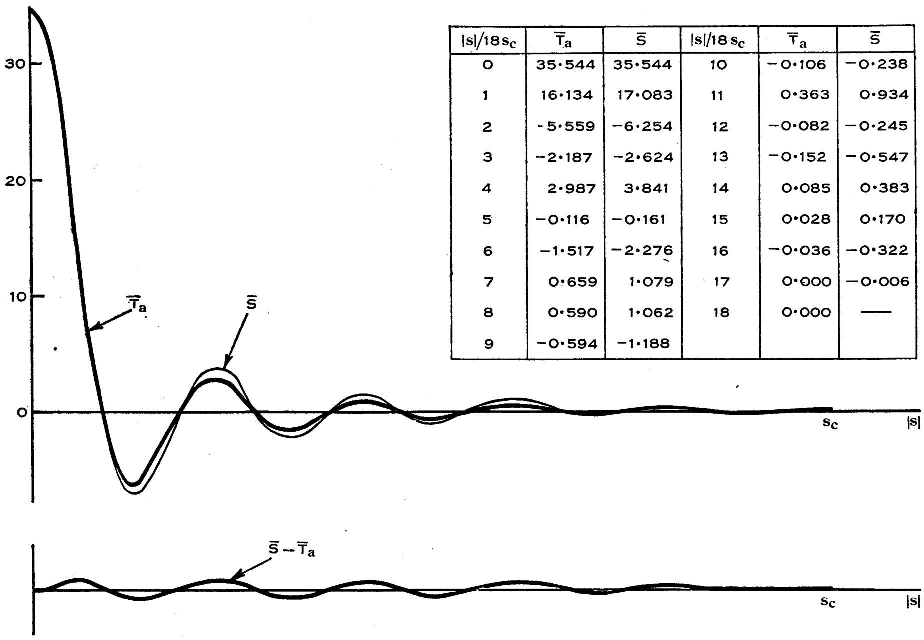

$\lvert s\rvert/18s_c$	$\bar{T}_a$	$\bar{S}$	$\lvert s\rvert/18s_c$	$\bar{T}_a$	$\bar{S}$
0	35·544	35·544	10	−0·106	−0·238
1	16·134	17·083	11	0·363	0·934
2	-5·559	−6·254	12	−0·082	−0·245
3	−2·187	−2·624	13	−0·152	−0·547
4	2·987	3·841	14	0·085	0·383
5	−0·116	−0·161	15	0·028	0·170
6	−1·517	−2·276	16	−0·036	−0·322
7	0·659	1·079	17	0·000	−0·006
8	0·590	1·062	18	0·000	——
9	−0·594	−1·188			

Fig. 12.—Distribution across the quiet Sun (Christiansen and Warburton 1953). The spectra of the observed distribution $\bar{T}_a$ and the principal solution $\bar{S}$ (above) and the difference between them (below).

The data T_a should be free from Fourier components of period shorter than φ_c, but the reduction processes intervening between the actual records and the adopted T_a, especially the subtraction of sunspot effects, might well introduce high frequencies. In the present case it was found that no correction for high frequencies needed to be made. In the following work we therefore adopt for our observed distribution the band-limited function defined by $T_a(\Phi)$, with Φ integral.

(b) *Restoration and the Spectrum*

We now attempt restoration by using the Fourier transforms of the two functions $\mathbf{A}$ and T_a. The Fourier transform of $\mathbf{A}(\varphi)$ is the triangular function

$$\begin{aligned} \bar{\mathbf{A}}(s) &= 1 - |s/s_c|, \qquad |s| < s_c, \\ &= 0, \qquad\qquad\quad\ |s| > s_c. \end{aligned}$$

The transform of T_a must be computed numerically. By our previous results, we may compute instead the transform of $\text{III}(\Phi)T_a$, and the Fourier integral then reduces *without approximation* to a summation of products. For each value of s there are 18 products as only 18 of the sequence of numbers defining T_a are non-zero. The transform of T_a, shown by the heavy curve in Figure 12, is oscillatory and decays to zero amplitude at the cut-off frequency s_c. (For reference the calculated values have been tabulated on the figure.)

TABLE 3

THE BRIGHTNESS DISTRIBUTION ACROSS THE QUIET SUN AT 21 CM (CHRISTIANSEN AND WARBURTON 1953). THE OBSERVED DISTRIBUTION T_a AND THE PRINCIPAL SOLUTION S

Φ	T_a	S	Φ	T_a	S	Φ	T_a	S
0	1·000	1·018		1·005		13	0·115	0·084
	1·000		7	1·005	1·024		0·087	
1	1·001	1·019		1·005		14	0·064	0·027
	1·001		8	1·004	1·036		0·047	
2	1·001	1·020		1·004		15	0·034	0·012
	1·002		9	1·002	1·089		0·024	
3	1·002	1·022		0·966		16	0·015	—0·007
	1·003		10	0·854	0·995		0·008	
4	1·003	1·024		0·680		17	0·004	—0·013
	1·003		11	0·490	0·440		0·000	
5	1·004	1·029		0·324		18	0·000	—0·014
	1·004		12	0·212	0·120		0·000	
6	1·004	1·028		0·153		19	0·000	—0·011

From $\bar{T}_a$ and $\bar{\mathbf{A}}$, $\bar{S}$ may be calculated by division. It is shown as the light curve in Figure 12. The difference curve $\bar{S}-\bar{T}_a$ shows the spectral distribution of the correction applied. The amplitudes of the Fourier components near the cut-off frequency are small, even after restoration.

To obtain the principal solution S it is now necessary to transform $\bar{S}$. Unfortunately the distribution S is not of finite extent, so that values of $\bar{S}$ at discrete intervals do not fully define $\bar{S}$. It is therefore necessary to know $\bar{S}$ at sufficiently small intervals of s to permit evaluation of the transform of $\bar{S}$ by numerical integration. On the other hand the Fourier integral need be evaluated at discrete intervals only. However, the labour involved in establishing $\bar{S}$ and transforming it is formidable. For interest we show by the heavy line in Figure 13 the result of transforming $\text{III}(18s/s_c)\bar{S}(s)$, that is, substituting for the Fourier integral of $\bar{S}$ a summation based on the 18 spot values of $\bar{S}$ given on Figure 12. The oscillations A, B, C prove to be spurious and arise from the use of too coarse an interval of s.

(c) *Successive Substitutions*

Restoration of T_a by the method of successive substitutions is illustrated in Figure 14. The figure shows T_a, with the limits of uncertainty indicated by shading; $A*T_a$; the successive corrections ε_1, ε_2, ε_3; and the corresponding restorations T_1, T_2, T_3. All the smoothing processes were computed using discrete values of the variables. From the three successive stages of restoration which are illustrated it may be seen that the corrections rapidly drop below the significant level. If T_3 is tested by forming $\mathbf{A}*T$, it is found to differ from T_a by ε_4 which is so small that $\mathbf{A}*T_3$, if plotted to the scale of Figure 14, would barely be distinguishable from T_a.

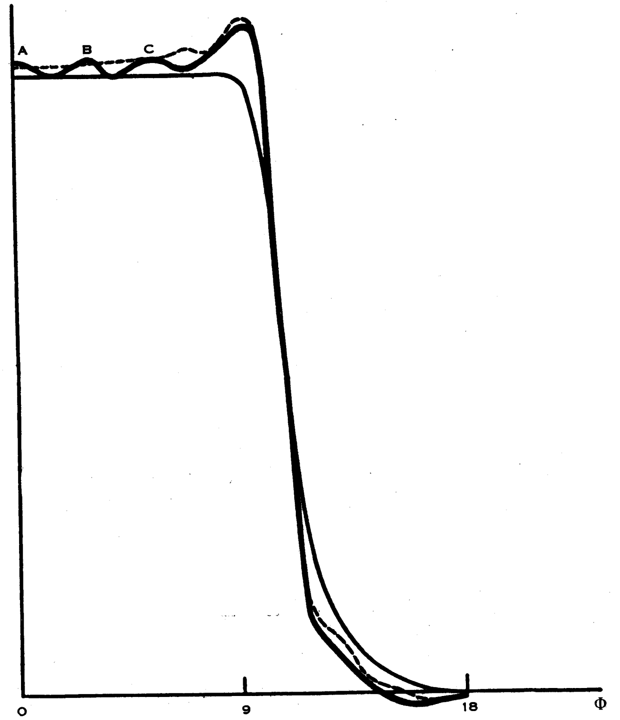

Fig. 13.—The observation distribution T_a (thin curve), the principal solution S (dotted curve), and an approximation to the principal solution obtained by restoring the transform of T_a (heavy curve).

It is not necessary in practice to obtain all the curves plotted in Figure 14, which was constructed simply to illustrate the process. Using the method outlined in Section VIII, T_3 may be obtained directly from T_a in one step.

In order to ascertain the principal solution with some accuracy, for the purpose of checking different proposals for approximating to it, we have carried the process to the 11th stage. The distribution so obtained is labelled S in Table 3 and is plotted as a dotted curve in Figure 13. One may verify that it is in fact the principal solution by scanning it with the aerial pattern. The result agrees with T_a to within one unit in the last decimal place at all integral values of Φ. The values of S between the tabulated values are to be understood as those given by the method of interpolation described in Section VI; consequently S is free from frequencies beyond s_c. The order of accuracy of this determination of S is of course much better than the 20 or 30 units in the last decimal which the accuracy of the observations would justify.

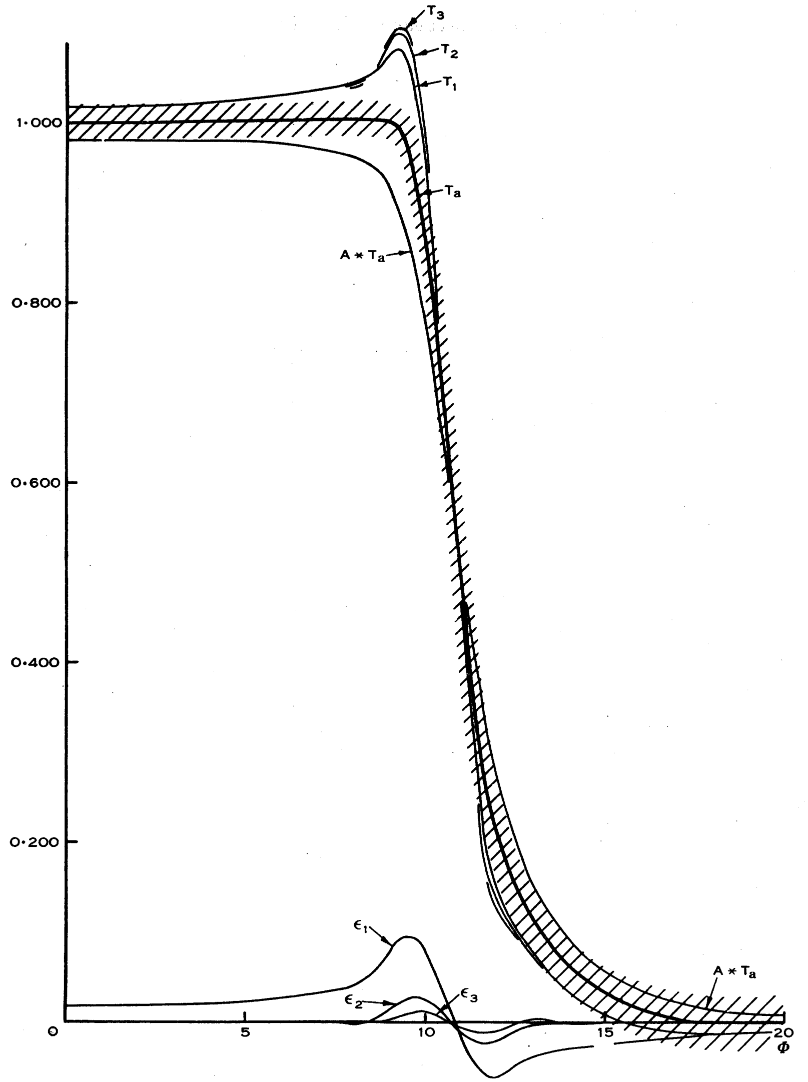

Fig. 14.—The observed distribution T_a, the successive corrections ε_1, ε_2, ε_3, and the successive restorations T_1, T_2, T_3.

X. References

Bolton, J. G., and Westfold, K. C. (1950).—Galactic radiation at radio frequencies. I. 100 Mc/s survey. *Aust. J. Sci. Res.* A **3**: 19.

Booker, H. G., and Clemmow, P. C. (1950).—The concept of an angular spectrum of plane waves, and its relation to that of polar diagram and aperture distribution. *Proc. Instn. Elect. Engrs.* III **97**: 11.

BOOKER, H. G., RATCLIFFE, J. A., and SHINN, D. H. (1950).—Diffraction from an irregular screen with applications to ionospheric problems. *Phil. Trans.* **242**: 579.

BROWN, R. H., and HAZARD, C. (1953).—A model of the radio-frequency radiation from the Galaxy. *Phil. Mag.* **44**: 939.

BURGER, H. C., and VAN CITTERT, P. H. (1932).—Wahre und scheinbare Intensitätsverteilung in Spektrallinien. *Z. Phys.* **79**: 722.

BURR, E. J. (1955).—Sharpening of observational data in two dimensions. *Aust. J. Phys.* **8** (in press).

CHRISTIANSEN, W. N. (1953).—A high-resolution aerial for radio astronomy. *Nature* **171**: 831.

CHRISTIANSEN, W. N., and WARBURTON, J. A. (1953).—The distribution of radio brightness over the solar disk at a wavelength of 21 centimetres. II. The quiet Sun—one-dimensional observations. *Aust. J. Phys.* **6**: 262.

VAN CITTERT, P. H. (1931).—Zum Einfluss der Spaltbreite auf die Intensitätsverteilung in Spektrallinien. *Z. Phys.* **69**: 298.

DOETSCH, G. (1937).—" Theorie und Anwendung der Laplacetransformation." (Springer: Berlin.)

FELLGETT, P. B., and SCHMEIDLER, F. B. (1952).—On the sharpening of observational data with special application to the darkening of the solar limb. *Mon. Not. R. Astr. Soc.* **112**: 445.

HEAVISIDE, O. (1922).—" Electromagnetic Theory." Vol. 2, p. 116. (Benn: London.)

HEY, J. S., PARSONS, S. J., and PHILLIPS, J. W. (1948).—An investigation of galactic radiation in the radio spectrum. *Proc. Roy. Soc.* A **192**: 425.

VAN DE HULST, H. C. (1941).—The determination of the true profile of a spectral line. *B.A.N.* **9**: 225.

VAN DE HULST, H. C. (1946).—Generalization of some methods for solving an integral equation of the first kind. *B.A.N.* **10**: 75.

LOVITT, W. V. (1950).—" Linear Integral Equations." (Dover: New York.)

O'BRIEN, P. A. (1953).—The distribution of radiation across the solar disk at metre wavelengths. *Mon. Not. R. Astr. Soc.* **113**: 597.

PATERSON, M. S. (1950).—Calculation of the correction for instrumental broadening in X-ray diffraction lines. *Proc. Phys. Soc.* A **63**: 477.

PIDDINGTON, J. H. (1951).—The origin of galactic radio-frequency radiation. *Mon. Not. R. Astr. Soc.* **111**: 45.

SHANNON, C. E. (1949).—Communication in the presence of noise. *Proc. Inst. Radio Engrs.* **37**: 10.

SMERD, S. F. (1950).—Radio-frequency radiation from the quiet Sun. *Aust. J. Sci. Res.* A **3**: 34.

SMITH, F. G. (1952).—The measurement of the angular diameter of radio stars. *Proc. Phys. Soc. Lond.* B **65**: 971.

SNEDDON, I. N. (1951).—" Fourier Transforms." (McGraw-Hill: New York.)

STOKES, A. R. (1948).—A numerical Fourier-analysis method for the correction of widths and shapes of lines on X-ray powder photographs. *Proc. Phys. Soc.* **61**: 382.

TRUMPLER, R. J., and WEAVER, H. F. (1953).—" Statistical Astronomy." (Univ. California Press.)

WASER, J., and SCHOMAKER, V. (1953).—Fourier inversion of diffraction data. *Rev. Mod. Phys.* **25**: 671.

WOODWARD, P. M., and LAWSON, J. D. (1948).—The theoretical precision with which an arbitrary radiation-pattern may be obtained from a source of finite size. *J. Instn. Elect. Engrs.* III **95**: 363.